Oblique laser incidence to select laser-generated acoustic modes

Samuel Raetz, Thomas Dehoux, Bertrand Audoin

Oblique laser incidence to select laser-generated acoustic modes

2011 J. Phys.: Conf. Ser. 278 012030

(http://iopscience.iop.org/1742-6596/278/1/012030)

Journal of Physics: Conference Series **278** (2011) 012030 doi:10.1088/1742-6596/278/1/012030

Oblique laser incidence to select laser-generated acoustic modes

S Raetz, T Dehoux and B Audoin

Université de Bordeaux, Laboratoire de Mécanique Physique, UMR CNRS 5469, France

E-mail: samuel.raetz@u-bordeaux1.fr

Abstract. The purpose of this paper is to study the effect of a non-normal optical penetration due to an obliquely incident laser source. It is shown that the loss of symmetry due to such a penetration influences specific bulk acoustic modes. For a given detection position, increase in shear wave amplitude is obtained by orienting the incident laser source.

1. Introduction

Since the first quantitative approaches in the 60's [1], a large number of studies has been conducted to better understand the generation of laser-generated acoustic waves. Models for the acoustic generation in the thermoelastic regime, taking into account the optical penetration of the source [2] or the effect of source width [3], were developed. A more general approach based on Green's function formalism also included thermal diffusion in the medium [4]. These works have dealt with the modeling of a circular spot of laser illumination. However, modeling of the acoustic field generated by a line source is of interest, since the signal-to-noise ratio may be increased in this experimental situation [5].

All the works cited above assume a normal incidence of the laser beam with respect to the illuminated surface of the sample. The purpose of this paper is to analyse the effects of oblique incidence on acoustic waves generated by a line-focused laser source. We present a theoretical model accounting for the effects of optical penetration, finite width of the beam and pulse duration of the laser source. The absorbed energy density is first calculated by solving Maxwell's equations. Then the thermoelastic equations are solved to obtain the displacement field through a semi-analytical calculation based on a double Fourier transform in space and time. It is shown that oblique incidence increases shear wave amplitude. Changes of the longitudinal waveforms are also discussed.

2. Volume source model for oblique incidence

2.1. Electromagnetic energy density distribution

A plate of finite thickness with parallel-sided slab of an absorbing medium is considered from here on in this paper. The thickness is assumed to be large compared to the optical penetration depth. A Schott NG1 glass film of thickness h = 2.5 mm is considered for calculations. The refractive index is n = 1.51, and the attenuation index is $\kappa = 3.39\ 10^{-4}$, corresponding to an optical penetration length of $1/\beta$ = 0.25 mm for normal incidence, β being the attenuation coefficient.

In order to determine the amount of energy deposited by the laser in the volume of the sample, Maxwell equations are solved [6]. A monochromatic electromagnetic plane wave of frequency ω is considered and, by convolving the solution with a spatial Gaussian profile, the actual spatial shape of the laser beam is obtained. Let θ_i be the incidence angle formed by the incident wave vector $\mathbf{k_i}$ and the direction normal to the surface of the sample $\mathbf{x_1}$ (see figure 1). It is convenient to assume that the incident electric field $\mathbf{E_i}$ is perpendicularly polarized:

$$\mathbf{E_i} = A_\perp \, \mathrm{e}^{-j(\omega t - \mathbf{k_i}\cdot\mathbf{r})} \, \mathbf{x_3} \;\text{ with }\; \mathbf{k_i} = k_i \left(\cos\theta_i \mathbf{x_1} + \sin\theta_i \mathbf{x_2}\right). \tag{1}$$

t, $\mathbf{r}$ and $A_\perp$ are the time, position vector and the amplitude of $\mathbf{E_i}$, respectively. Since the sample thickness is large compared to the optical penetration depth, optical reflections at the second interface, $x_1 = h$, of the sample are not considered. Because the sample is absorbing, the optical wave vector of the transmitted waves $\mathbf{k_t}^*$ is complex. Optical phase continuity at the interface implies that $\mathbf{k_t}^*.\mathbf{x_2}$ is real. From the continuity for electric and magnetic fields at the interface, one can deduce relations between $A_\perp$ and the amplitude of the transmitted electric wave $T_\perp{}^*$. This expression is written in terms of complex optical index $n^* = n + j\kappa$ using the optical dispersion relation in an isotropic medium [6]:

$$T_\perp^* = \frac{2\cos\theta_i}{\cos\theta_i + (n + j\kappa)\cos\theta_t} A_\perp = \Upsilon^* A_\perp , \tag{2}$$

where Υ^* is the complex transmission coefficient in amplitude.

The local law of the electromagnetic conservation of energy leads to the following expression of energy density in the sample ($x_1 \geq 0$):

$$Q(x_i,t) = \beta n \left|\Upsilon^*\right|^2 I_0 \, \mathrm{e}^{-\beta x_1} \, g(x_1,x_2) \, f(t), \forall x_1 \geq 0 . \tag{3}$$

$I_0 = cA_\perp{}^2/8\pi$ is the incident intensity of the laser beam and $\beta = 2\omega\kappa\cos\theta_t/c$ is the attenuation factor, where c is the light speed in vacuum. g and f represent the spatial and temporal Gaussian distribution of the source, respectively. Assuming a pulse width of 5 ns and a width at half-height of the space distribution of 12.5 μm, $Q(x_i,0)$ is shown in figures 2(a) and (b) for $\theta_i = 0°$ and $\theta_i = 50°$, respectively. A clear effect of the incidence is observed due to the dependence of β and Υ^* on the refracted angle θ_t [and therefore on θ_i, see equations 2 and 3]. Another change in this expression of Q, compared with previous models, is the dependence of g on the x_1 coordinate due to oblique incidence. To investigate the effect, it can be convenient to express g as a convolution product between a Gaussian function G and the impulse function δ:

$$g(x_1,x_2) = \delta(x_2 - x_1\tan\theta_t) * G(x_2) . \tag{4}$$

Consequently, the spatial location of the energy along the refracted direction of the laser beam, introduced by $\delta(x_2 - x_1\tan\theta_t)$, should cause visible change on acoustic waves.

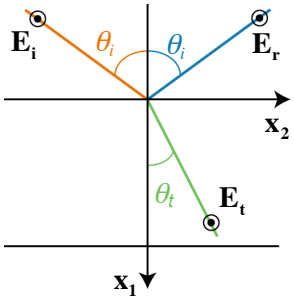

Figure 1. Geometry

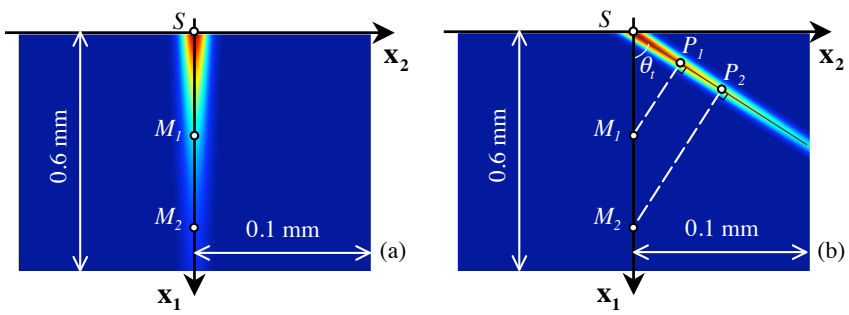

Figure 2. Energy density for (a) $\theta_i = 0°$ and (b) $\theta_i = 50°$

2.2. Displacement field

From the calculated energy density, see 2.1, the temperature distribution T is obtained solving the heat equation. Since the thermal diffusion length is shorter than the optical penetration length in the material of interest at the time scale of the acoustic wave generation, thermal diffusion is neglected. The volume source of expansion is conducted by the optical penetration depth. The heat equation is reduced to:

$$\rho C_p \frac{\partial T}{\partial t} = Q\left(x_i, t\right), \tag{5}$$

where ρ is the density of the material and C_p is the specific heat. The temperature field is then obtained by integrating the equation above:

$$T\left(x_i, t\right) = \frac{\beta n \left|\Upsilon^*\right|^2 I_0}{\rho C_p} \mathrm{e}^{-\beta x_1} g\left(x_1, x_2\right) \int_0^t f\left(u\right) du \;\forall x_1 \geq 0 \,. \tag{6}$$

The wave equation is:

$$\nabla \cdot \left(\left[C\right] : \nabla \mathbf{u}\right) - \rho \frac{\partial^2 \mathbf{u}}{\partial t^2} = \left[C\right] : \left[\alpha\right] \nabla T \;, \tag{7}$$

where $\mathbf{u}$ is the displacement vector, $[C]$ the stiffness tensor and $[\alpha]$ the thermal dilatation tensor. A semi-analytical solution is computed, adapting the calculation scheme detailed in Ref. [7].

The effects on the acoustic generation of the dependence of β and Υ^* with respect to incidence angle and of the dependence of g on x_1 are presented and discussed in the following section.

3. Results

Normal displacements within the sample volume along $\mathbf{x_1}$ are plotted vs. time in figure 3. The observation points M_i are located under the source impact point S at the surface (see figure 2). Longitudinal acoustic waves are generated by the in-depth volume source of expansion. Their reflections at the free surface yield bulk longitudinal and shear waves. Arrival times are equal in both the normal and 50° incidence configurations. The amplitude of the normal displacement is weaker in the case of an incident (50°) source due to the decrease of the transmission coefficient $\left|\Upsilon^*\right|$ with increasing angle of incidence (equation 2).

Upon oblique incidence, the first longitudinal wave reaching point M_i was generated near the orthogonal projection P_i of this point on the refracted direction [see figure 2(b)]. A step at the beginning of the signal is thus observed, which does not exist in the well known exponential profile of the so-called precursor for normal incidence [8]. This step is obviously less noticeable when the distance between S and M_i increases.

Normal displacements at different points on the rear surface, $x_1 = h$, are displayed in figure 4(a). Film thickness h is large enough to observe longitudinal and transverse contributions to the displacement separately. The longitudinal wave is denoted (L) in figure 4(a) whereas the shear wave is denoted (T). Shear wave amplitude is more sensitive to the incidence angle than the longitudinal mode [figure 4(a)]. In order to illustrate this effect, shear wave amplitudes in both configurations (normal and oblique incidence) are normalized with respect to the absorbed laser intensity $n\left|\Upsilon^*\right|^2 I_0$ to compensate for the fall in transmission coefficient $\left|\Upsilon^*\right|$. With $\theta_i = 50°$, thus $\theta_t \sim 30°$, it appears in figure 4(c) that, for the same absorbed energy, the shear wave amplitude is larger in the oblique incidence configuration. Furthermore the maximum of amplitude is shifted compared to the one at normal incidence.

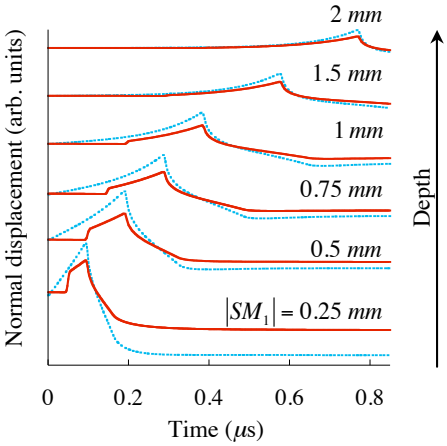

Figure 3. Normal displacement at different depths for $\theta_i = 0°$ (dash) and $\theta_i = 50°$ (solid) with $1/\beta = 0.25$ mm

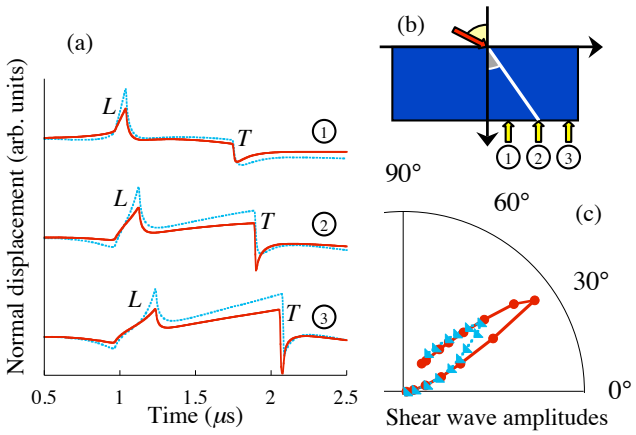

Figure 4. (a) Normal displacement at three detection points shown in (b), and (c) shear wave amplitudes in polar coordinates normalized with respect to the absorbed laser intensity for $\theta_i = 0°$ (dash) and $\theta_i = 50°$ (solid)

4. Perspectives

A model of the volume source of expansion for oblique incidence has been presented and effects on the thermal normal gradient have been discussed. We have demonstrated that the longitudinal waveforms are changed and that the shear wave amplitude can be increased due to oblique incidence of the laser beam, and thus a specific mode can be enhanced by changing the incidence angle of the source. These predictions will be compared with a pump-probe experiment using nanosecond laser pulses to generate acoustic waves in samples made of colored glasses.

References

[1] Lee R E and White R M 1968 *Appl. Phys. Letters* **12** 12-14
[2] Dewhurst R J, Hutchins D A, Palmer S B and Scruby C B 1982 *J. Appl. Phys.* **53** 4064-71
[3] Scruby C B, Dewhurst R J, Hutchins D A, Palmer S B 1980 *J. Appl. Phys.* **51** 6210-16
[4] Doyle P A 1986 *J. Phys.* D*: Appl. Phys.* **19** 1613-23
[5] Arias I and Achenbach J D 2003 *Int. J. Solids Struct.* **40** 6917-35
[6] Born M and Wolf E 2005 *Principles of Optics - 7th ed.* (Cambridge University Press)
[7] Audoin B, Meri H and Rossignol C 2006 *Phys. Rev.* B **74** 214304
[8] Dubois M, Enguehard F and Bertrand L 1994 *Phys. Rev* . E **50** 1548-51